Journal of Materials Chemistry A

Accepted Manuscript

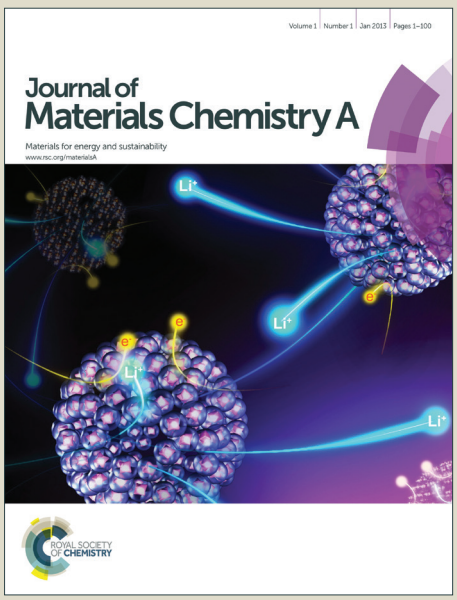

ROYAL SOCIETY OF CHEMISTRY

www.rsc.org/materialsA

Journal of Material Chemistry A RSCPublishing

ARTICLE

Binder-free Rice Husk-based Silicon-Graphene Composite as Energy Efficient Li-ion Battery Anodes

Cite this: DOI: 10.1039/x0xx00000x

Received 00th January 2012,
Accepted 00th January 2012

DOI: 10.1039/x0xx00000x

www.rsc.org/

Deniz P. Wong[a,b,c], Rangaraj Suriyaprabha[d], Rathinam Yuvakumar[d], Venkatachalam Rajendran[d], Yit-Tsong Chen[c,f], Bing-Joe Hwang[e], Li-Chyong Chen[a*] and Kuei-Hsien Chen[f*]

Rice husks, often neglected and considered as waste, contain constituents that could be of potential use in advanced material applications. In this study, rice husks were used as a source of silicon dioxide for the synthesis of silicon nanoparticles (Si NPs) through magnesiothermic reduction process. The Si NPs were further used to prepare a binder-free composite system comprised of Si NPs and graphene as an anode material for lithium ion battery system (LiBs). The composite system fabricated from rice husk-based Si NPs (RH-Si NPs) yielded an initial capacity of 1000 mAh/g at high applied current density of 1000 mA/g. This study opens up the use of waste materials such as rice husk as a sustainable source of key components in advanced technology applications.

Introduction

Rice (*Oryza sativa*) is a major staple food in most countries in the world. As such, there is a constant need to produce rice in a steady basis in order to meet the demands of the growing population of the world. In recent years, the world consumed 470 million metric ton of rice.[1] With it, several million tons of corresponding rice husk is also produced. Despite the application of rice husks in construction materials,[2] fertilizers[3] and fuel,[4, 5] they are generally considered as waste. Although these husks naturally decompose, the sheer amount available makes it ideal to utilize such waste product into potential technologies that can elevate our living conditions. In this study, we utilized rice husk as a raw material for lithium ion battery related applications.

Rice husk contains high amounts of silicon dioxide which can, in turn, be a useful source of silicon. It contains around 10 – 20% of silicon dioxide depending on the soil in which the stalks grow.[6] There are various methods to extract silicon dioxide from the rice husk including variation of acid pre-treatment[7, 8] and subsequent pyrolysis.[9, 10] Different sources of rice husk also influence the properties of the silicon dioxide extracted.[11, 12] Oftentimes, silicon dioxide extracted from the husk comes in nanoscale morphology. Banerjee *et al.* have shown that it is possible to convert silicon dioxide to silicon through a magnesiothermic reduction process[13] while maintaining the relative morphology of the initial material. Since the reported reaction was done in a relatively low temperature (600 ^{0}C)[13], sintering of Si NPs into bulk scale can be minimized. This opens up the possibility of producing Si NPs from the silicon dioxide nanoparticles.[14] Moreover, this also creates the opportunity to obtain cheaper source of Si NPs for applications in lithium ion battery systems.[15-17]

Si NPs are an attractive anode material for the next generation lithium ion battery.[18] Theoretically, Si reacts with the most number of lithium ions during alloying which delivers a high specific capacity (3579 mAh/g at room temperature) which is an order of magnitude higher than the current graphite-based anodes. However, Si-based materials in a LiBs system face the problem of volume expansion caused by different stages of alloying formation during the charge-discharge cycle[19] and the intrinsically poor conductivity of Si.[20] To mitigate this problem, composite-based approaches have been demonstrated.[21]

Graphene, being a 2D-based material, can act as a buffering matrix and electron conductor for Si in LiBs.[22, 23] Interestingly, most recent studies on such composite-based system still use additives including binders and conductive materials such as active carbon.[24, 25]

In this study, we took a step further by adopting a binder-free composite approach to incorporate the rice husk-based Si NPs (RH-Si NPs) for battery testing. This would reduce the materials needed in fabricating our battery electrodes such as elimination of the traditional copper foil and organic binder. As such, the corresponding cost of the battery electrodes is also reduced. In addition, we have also adopted a solvent-exchange process that helps improve the interaction of Si NPs in graphene oxide (GO) solution. The combination of low-cost material resources and the improved material's processing technique opens up new alternative route in Li ion battery fabrication and testing.

Experimental Methods

Fig. 1 shows the flow diagram of the process used in this study. The process of extracting SiO_2 nanoparticle from rice husk is a modification of the one reported by Kalapathy *et al*.[8] The process involves the following extraction procedures:

$$\text{RHA } (SiO_2)\ (s) + 2\ NaOH\ (aq) \rightarrow Na_2SiO_3\ (s) + H_2O\ (l) \quad (1)$$

$$Na_2SiO_3\ (s) + H_2SO_4\ (aq) \rightarrow SiO_2\ (s) + Na_2SO_4\ (aq) + H_2O\ (l) \quad (2)$$

Briefly, after ashing the rice husk, the ash was subjected to basic solution by adding sodium hydroxide (NaOH) to extract SiO_2 in the form of sodium silicate. The silicate was then separated by filtration, followed by neutralization to pH 7 by titration with concentrated sulfuric acid. The SiO_2 precipitate was formed as the pH was decreased to below 10. The SiO_2 nanoparticles were then filtered, washed with water and sintered at 550 ^oC for 2 hours prior to the subsequent reduction process.

To convert the SiO_2 nanoparticles to Si nanoparticles, a magnesiothermic reduction process was used.[13, 27]

$$SiO_2\ (s) + 2\ Mg\ (g) \rightarrow Si\ (s) + 2\ MgO\ (s) \quad (3)$$

$$\Delta_r G = -399.20\ \text{kJ/mol (at 700 } ^oC)^{28}$$

The oxide particles were mixed with magnesium powders at a mole ratio of 1:2. The mixed reactants were then placed in a stainless steel reactor vessel and into a quartz-tube furnace in an Ar atmosphere at 700 ^oC for 3 hours. The products were then washed with 1 M HCl solution to remove the magnesium oxide by-product. After filtering the sample, Si NPs were then subjected to 5% HF washing to remove the unreacted SiO_2 NPs and surface oxide. The Si NPs were then filtered, washed several times and dried in vacuum overnight.

In order to improve the dispersion of Si NPs in aqueous media, solvent exchange process was applied, which has been reported elsewhere.[26] Briefly, 1-methyl-2-pyrrolidone was added to Si NPs, followed by one-hour ultrasonic agitation and ultra-high centrifugation to extract the Si NPs. The solvent was removed and GO solution was added to form the homogeneous composite mixture. The aforementioned GO was obtained using a modified Hummer's method[29, 30](S1†).

After obtaining a homogeneous composite solution from the solvent exchange process, the paper was obtained by vacuum filtration of the solution on an alumina filter paper (Whatman Anodisc). After drying, the paper was easily peeled from the filter paper. The sample was subjected to thermal annealing at 700 ^oC in argon atmosphere to convert the graphene oxide into more conductive reduced graphene oxide to improve the conductivity of the composite paper following the procedure of Zhao *et al*.[23] The paper was then cut into the desired shape to be used as an electrode for lithium ion battery testing. The thickness of the paper was measured to be around 30-40 μm from the cross-section SEM image shown in Fig. S2†.

Thermal gravimetric analysis (TGA) with differential thermal analysis (DTA) experiments was done using Perkin-Elmer Diamond. X-ray powder diffraction patterns (XRD) were done using Bruker D8 Advance. The morphology observation and elemental analysis were done using a field emission scanning electron microscope (SEM) (JEOL JSM-6700F) attached with an energy dispersive spectrometer (EDS) (Oxford Instruments) while transmission electron microscopic images were done using JEOL TEM-2100 FE-TEM). Raman spectra were obtained using a confocal Raman spectrometer (Jovin Yvon Horiba 800UV) with a 633 nm He–Ne laser as the excitation source. The battery test was done by fabricating a CR2032 coin cell using 1 M $LiPF_6$ in EC/DMC (1:1 v/v) by Tomiyama as electrolyte and glass fiber membranes from Whatman was used as separator. The mass of the RH-Si NPs composite electrode used per coin cell was maintained at around 0.25 mg. Pure lithium metal foil was used as the counter electrode and assembly of the battery system was done in an argon-filled glove box. The measurement was performed using a CHG-5500C system fixed at a voltage window between 0.01 and 1.5 V at room temperature. Cyclic voltammetry (CV) experiments were done using Solartron 1287 system while the sheet resistance was obtained using a four-point probe measuring system.

Results and Discussion

The TGA and DTA data in Fig. 2 illustrate the combustion of carbon leaving behind SiO_2 component, indicating that rice husk mostly contains carbon materials. However, in a large scale extraction of rice husk, some carbon residue may remain on the surface of the oxide component. Thus, in this study, a base extraction procedure was adopted to obtain SiO_2 NPs.[31,32]

After obtaining the SiO_2 NPs, the magnesiothermic reduction process was used to convert the oxide material to Si NPs. Fig. 3 shows the evolution of the product at each stage of

the reduction process by monitoring the corresponding XRD spectra. Aside from magnesium oxide, magnesium silicide is also formed as a side product during the reaction. These two products are easily removed in the subsequent acid washing step, leaving behind Si NPs and some unreacted residual SiO_2 NPs which can be removed by HF washing. From the spectra, it is apparent that good crystallinity and purity of Si NPs was obtained. The grain size was approximated to about 70 nm based from the Scherrer's equation.

The Si NPs were combined with GO solution after undergoing the solvent exchange process as mentioned above. The process enabled us to produce a homogeneous solution of Si NPs in aqueous solution, avoiding the dispersion problem of Si NPs in the medium. The obtained Si NPs were then used for the composite system in battery applications.

After thermal annealing, the GO in the composite was converted into reduced GO to improve the conductivity of the paper. Initially, the conductivity of the paper is in the order of gigaohms per square, which was reduced to 6.72 ohms per square after the annealing treatment. SEM and TEM images (Fig. 4) shows Si NPs wrapped within the carbon matrix, yielding an improved interface contact from the two materials. This may help in the electron transport during battery testing. In addition, Fourier transformation of the high resolution TEM images also show that the crystallinity of Si NPs was preserved while evidence of improved crystallinity of GO matrix was produced after the thermal treatment. Fig. 5 also shows SEM-EDS maps of composite paper after thermal annealing. The maps indicate a homogeneous mix between Si and C components, with small amount of O which possibly arises from surface oxidation of both materials. The material was also characterized by XRD and Raman spectroscopy as illustrated in Fig. S3† showing the XRD pattern of Si NPs–GO paper from rice husk before and after thermal annealing. Prior to annealing, peak at around 10^o is observed on the composite paper which is typically indicative of the presence of GO.[33] Whereas, after the reduction process, the peak disappeared while the peaks associated with Si NPs remained.

This corroborates the results obtained from the Raman spectrum (Fig. S4†), in which the D band to G band ratio decreased after the reduction process indicating that the disordered carbon present is lessened and most likely converted to sp^2 bonds. EDS spectra also confirms the reduction of oxygen content after the thermal reduction process (Fig. S5†).

Since the composite paper thus fabricated can stand on its own without the need of a substrate, the material was directly tested for its battery performance. The added simplification also allows us to directly gauge the effect and quality of the Si NPs used for the study. Previously, polymer binders (polyvinylidene fluoride (PVDF), carboxymethyl cellulose (CMC) and etc.) and carbon additives (Super P) were needed in order to make an acceptable working coin cell.[34] Most groups still use such system since these materials help in the overall battery performance. Furthermore, additives such as vinylidene carbonate[35] can be added to the electrolyte to improve cycling stability of the battery. However, they may also mask some of the needed qualities (such as conductivity, required geometry, etc.) of the Si NPs that can help determine its applicability in lithium ion battery platform. The binder-free method allowed us to gauge our anode materials on the merit of the active materials' respective property without being compromised by the additive.

Fig. 6a shows the cycling performance of the rice husk based-Si NPs–rGO paper. The initially capacity was shown to be around 1000 mAh/g with initial coulombic efficiency of 70%. It should also be noted that higher specific capacity can be obtained when lower current (200mAh/g) was applied, whereas the cycling performance was performed using an applied current of 1000 mA/g, which is 3-4 times higher than those reported in the literature that have similar or slightly higher specific capacity.[36-38] Figure 6b shows the 1st cycle charge–discharge curve of the RH-Si NPs graphene composite under two different cycling rates. As expected, applying higher rate (1000 mA/g) delayed some of the necessary SEI formation required. This causes some losses in terms of specific capacity of the material. Nevertheless, we still demonstrated a high specific capacity (~1000 mAh/g) at applied rate of 1000 mA/g. Different cycling rates, ranging from 200 mA/g to 2000 mA/g, have been used to test the rate capability of our RH-Si NPs – GO paper (Fig. 6c). The results show that the electrode can withstand the effect of higher applied current density. The specific capacity is similar to its corresponding value at the same cycle number (compare Fig. 6a and 6c) regardless if the electrode underwent constant applied current (Fig. 6a) or applied current from 200 mA/g to 2000 mA/g, and back to 200 mA/g at certain fixed increments (Fig. 6c).

Lastly, cyclic voltammetry was used to probe the electrochemical reaction going on during the early stages of the lithium insertion and extraction (Fig. 6d). The cathodic peak can be observed at 600 mV during the first cycle (red color) which indicates the SEI formation. After the succeeding cycle, the peak decreases and saturates, indicating the stabilization of the SEI. The peaks associated with lithium insertion and extraction can correctly be assigned at 20 mV, 300 mV and 500 mV.[39] Furthermore, the anodic peaks associated to the lithium extraction process can be observed to broaden into one peak instead of the typical two peaks, which was attributed to the reaction with nanocrystalline phase in the anode material.

Conclusion

Incorporating the solvent exchange method[28] enables us to fabricate a homogeneous free-standing binder-free RH-Si NPs composite film. The film demonstrated good potential as high energy density anode material in a lithium ion battery system with an initial capacity of about 1000 mAh/g at a high current density of 1000 mA/g and maintained reasonable capacity after 30 cycles. These findings demonstrate the conversion of a waste material into a useful, dependable energy storage device which can pave the way into the viability of scavenging raw materials as potential source for future technological applications.

Acknowledgements

The author would like to thank Mr. J.M. Chou from NTUST for helping with the TEM and SEM work. This work was supported by the Taiwan International Graduate Program and grants from the Institute of Atomic Molecular Sciences, Academia Sinica, Center for Emerging Material and Advanced Devices, National Taiwan University and the National Science Council of Taiwan.

Notes and references

[a] *Center for Condensed Matter Sciences, and Center for Emerging Material and Advanced Devices, National Taiwan University, Taipei 10617, Taiwan*
[b] *Nanoscience and Technology Program, Taiwan International Graduate Program, Academia Sinica, Taipei 11529, Taiwan*
[c] *Department of Chemistry, National Taiwan University, Taipei 10617, Taiwan*
[d] *Center for Nanoscience and Technology, K. S. Rangasamy College of Technology, Tiruchengode – 637 215, Tamil Nadu, India*
[e] *Department of Chemical Engineering, National Taiwan University of Science and Technology, 43 Keelung Road, Section 4, Taipei 10617, Taiwan*
[f] *Institute of Atomic and Molecular Sciences, Academia Sinica, Taipei 10617, Taiwan*
Fax: +886- 2-336652xx; Tel: +886-2-33665231; E-mail: chenlc@ntu.edu.tw (L.C. Chen) or chenkh@pub.iams.sinica.edu.tw (K.H. Chen).

† Electronic Supplementary Information (ESI) available: Details on the synthesis of graphene oxide, XRD, Raman and EDS spectra of rice husk-based Si NPs-rGO composite. See DOI: 10.1039/b000000x/

1. F. A. Services, ed. U. S. D. o. Agriculture, United States, 2013.
2. G. Rodríguez de Sensale, *Cem. Concr. Compos.*, 2006, **28**, 158.
3. S. Kamenidou, T. J. Cavins and S. Marek, *Sci. Hortic.*, 2010, **123**, 390.
4. F. Duan, C.-S. Chyang, C.-W. Lin and J. Tso, *Bioresour. Technol.*, 2013, **134**, 204.
5. M. Fang, L. Yang, G. Chen, Z. Shi, Z. Luo and K. Cen, *Fuel Process. Technol.*, 2004, **85**, 1273.
6. S. Chandrasekhar, K. G. Satyanarayana, P. N. Pramada, P. Raghavan and T. N. Gupta, *J. Mater. Sci.*, 2003, **38**, 3159.
7. N. Yalcin and V. Sevinc, *Ceram. Int.*, 2001, **27**, 219.
8. Kalapathy, *Bioresour. Technol.*, 2002, **85**, 285.
9. T.-H. Liou, *Mater. Sci. Eng., A*, 2004, **364**, 313.
10. F. Adam, J. N. Appaturi and A. Iqbal, *Catal. Today*, 2012, **190**, 2.
11. V. B. Carmona, R. M. Oliveira, W. T. L. Silva, L. H. C. Mattoso and J. M. Marconcini, *Ind. Crops Prod.*, 2013, **43**, 291.
12. V. H. Le, C. N. H. Thuc and H. H. Thuc, *Nanoscale Res. Lett.*, 2013, **8**, 58.
13. H. D. Banerjee, S. Sen and H. N. Acharya, *Mater. Sci. Eng*, 1982, **52**, 173.
14. L. Sun and K. Gong, *Ind. Eng. Chem. Res.*, 2001, **40**, 5861.
15. A. Xing, S. Tian, H. Tang, D. Losic and Z. Bao, *RSC Adv.*, 2013, **3**, 10145.
16. N. Liu, K. Huo, M. McDowell, J. Zhao and Y. Cui, *Sci. Rep.*, 2013, **3**, 1919.
17. D. Jung, M. Ryou, Y. Sung, S. Park and J. Choi, *Proc. Nat. Acad. Sci.*, 2013, **110**, 12229.
18. U. Kasavajjula, C. Wang and A. J. Appleby, *J. Power Sources*, 2007, **163**, 1003.
19. B. A. Boukamp, *J. Electrochem. Soc.*, 1981, **128**, 725.
20. J. K. Lee, K. B. Smith, C. M. Hayner and H. H. Kung, *Chem. Comm.*, 2010, **46**, 2025.
21. A. Magasinski, P. Dixon, B. Hertzberg, A. Kvit, J. Ayala and G. Yushin, *Nat. Mater.*, 2010, **9**, 353.
22. S.-L. Chou, J.-Z. Wang, M. Choucair, H.-K. Liu, J. A. Stride and S.-X. Dou, *Electrochem. Comm.*, 2010, **12**, 303.
23. X. Zhao, C. M. Hayner, M. C. Kung and H. H. Kung, *Adv. Energy Mater.*, 2011, **1**, 1079.
24. S. Zhu, C. Zhu, J. Ma, Q. Meng, Z. Guo, Z. Yu, T. Lu, Y. Li, D. Zhang and W. M. Lau, *R. Soc. Chem. Adv.*, 2013, **3**, 6141.
25. M. Ge, J. Rong, X. Fang, A. Zhang, Y. Lu and C. Zhou, *Nano Res*, 2013, **6**, 174.
26. D. P. Wong, H.-P. Tseng, Y.-T. Chen, B.-J. Hwang, L.-C. Chen and K.-H. Chen, *Carbon*, 2013, **63**, 397.
27. Z. Bao, M. R. Weatherspoon, S. Shian, Y. Cai, P. D. Graham, S. M. Allan, G. Ahmad, M. B. Dickerson, B. C. Church, Z. Kang, H. W. Abernathy Iii, C. J. Summers, M. Liu and K. H. Sandhage, *Nature*, 2007, **446**, 172.
28. I. Barin, *Thermochemical Data of Pure Substances*, VCH Verlagsgesllschaft mbH, Federal Republic of Germany, 1995.
29. W. S. Hummers and R. E. Offeman, *J. Amer. Chem. Soc.*, 1958, **80**, 1339.
30. H.-C. Hsu, I. Shown, H.-Y. Wei, Y.-C. Chang, H.-Y. Du, Y.-G. Lin, C.-A. Tseng, C.-H. Wang, L.-C. Chen, Y.-C. Lin and K.-H. Chen, *Nanoscale*, 2013, **5**, 262.
31. R. Yuvakkumar, V. Elango, V. Rajendran and N. Kannan, *J. Exp. Nanosci.*, 2014, **9**, 272.
32. K. Saravanan, R. Yuvakkumar, V. Rajendran and P. Paramasivam, *Phase Transitions*, 2012, **85**, 1109.
33. L. Tang, Y. Wang, Y. Li, H. Feng, J. Lu and J. Li, *Adv. Funct. Mater.*, 2009, **19**, 2782.
34. V. Etacheri, R. Marom, R. Elazari, G. Salitra and D. Aurbach, *Energy Environ. Sci.*, 2011, **4**, 3243.
35. N. Ding, J. Xu, Y. Yao, G. Wegner, I. Lieberwirth and C. Chen, *J. Power Sources*, 2009, **192**, 644.
36. S. Xin, Y.-G. Guo and L.-J. Wan, *Accounts Chem. Res.*, 2012, **45**, 1759.
37. X. Zhou, Y.-X. Yin, L.-J. Wan and Y.-G. Guo, *Adv. Energy Mater.*, 2012, **2**, 1086.
38. S. Yang, G. Li, Q. Zhu and Q. Pan, *J. Mater. Chem.*, 2012, **22**, 3420.
39. B. Wang, X. Li, X. Zhang, B. Luo, M. Jin, M. Liang, S. A. Dayeh, S. T. Picraux and L. Zhi, *ACS Nano*, 2013, **7**, 1437.

Fig. 1 Flow diagram of the process used to convert rice husk into Si NPs and subsequent fabrication of the composite paper with GO solution and battery fabrication.

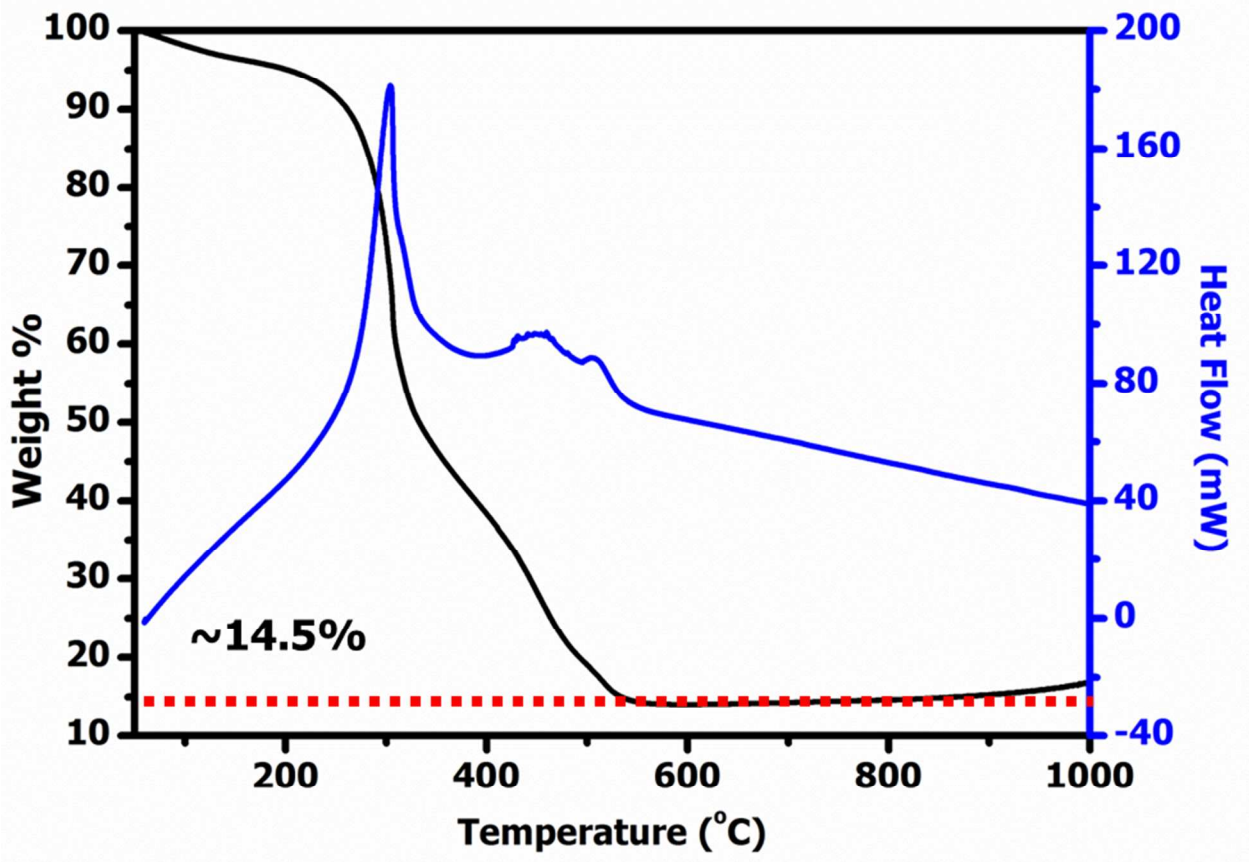

Fig. 2 DTA and TGA curves of Rice husk in argon (Ar) atmosphere

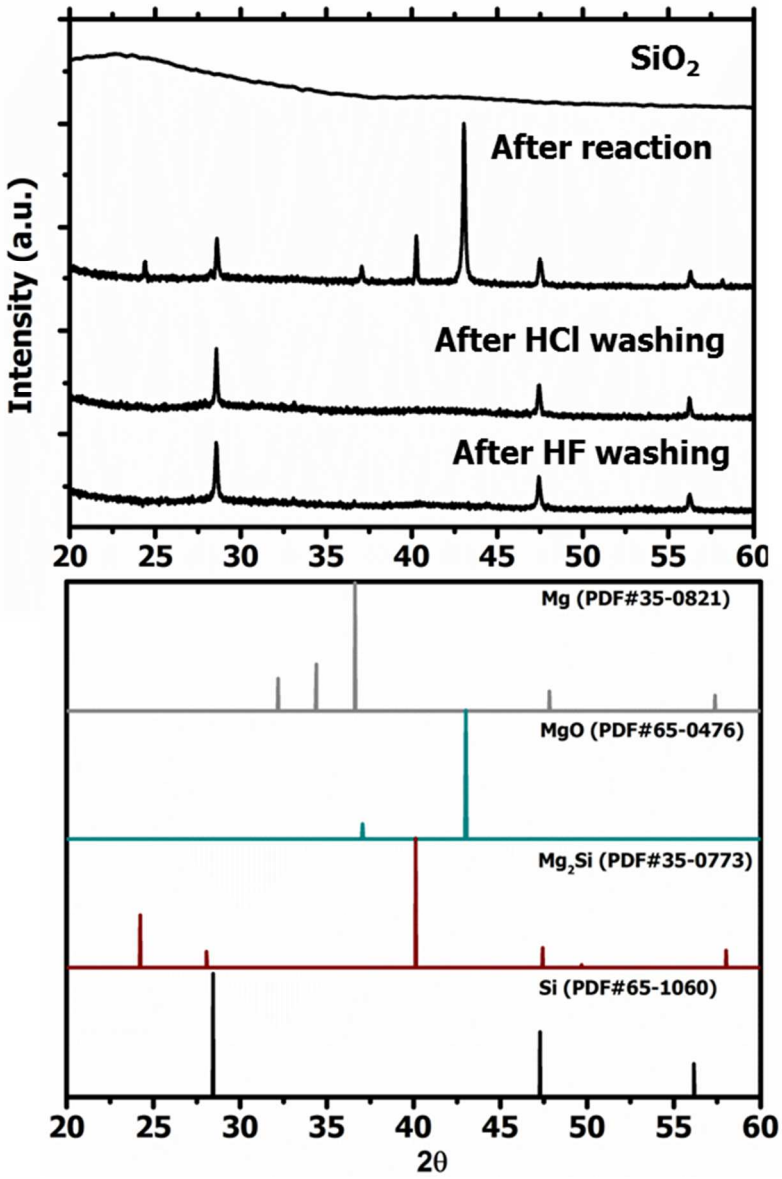

Fig. 3 XRD spectra of different products obtained at various stages of the reduction process until the formation of Si NPs after HF washing. The powder diffraction data of possible products formed in the reduction process are also listed.

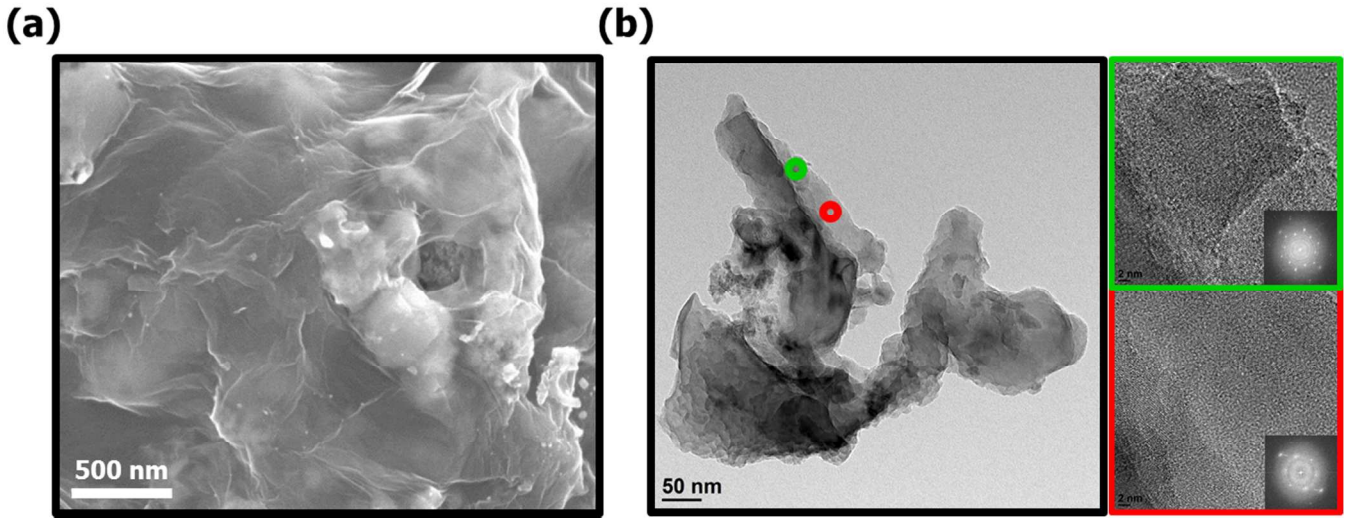

Fig. 4 An (a) SEM image of RH-Si NPs –rGO composite paper and (b) the corresponding TEM image of the material where the indicated colored circle corresponds to the high resolution image of the selected area (green for Si NPs with d-spacing of 3.1Å and red for graphene sheets.

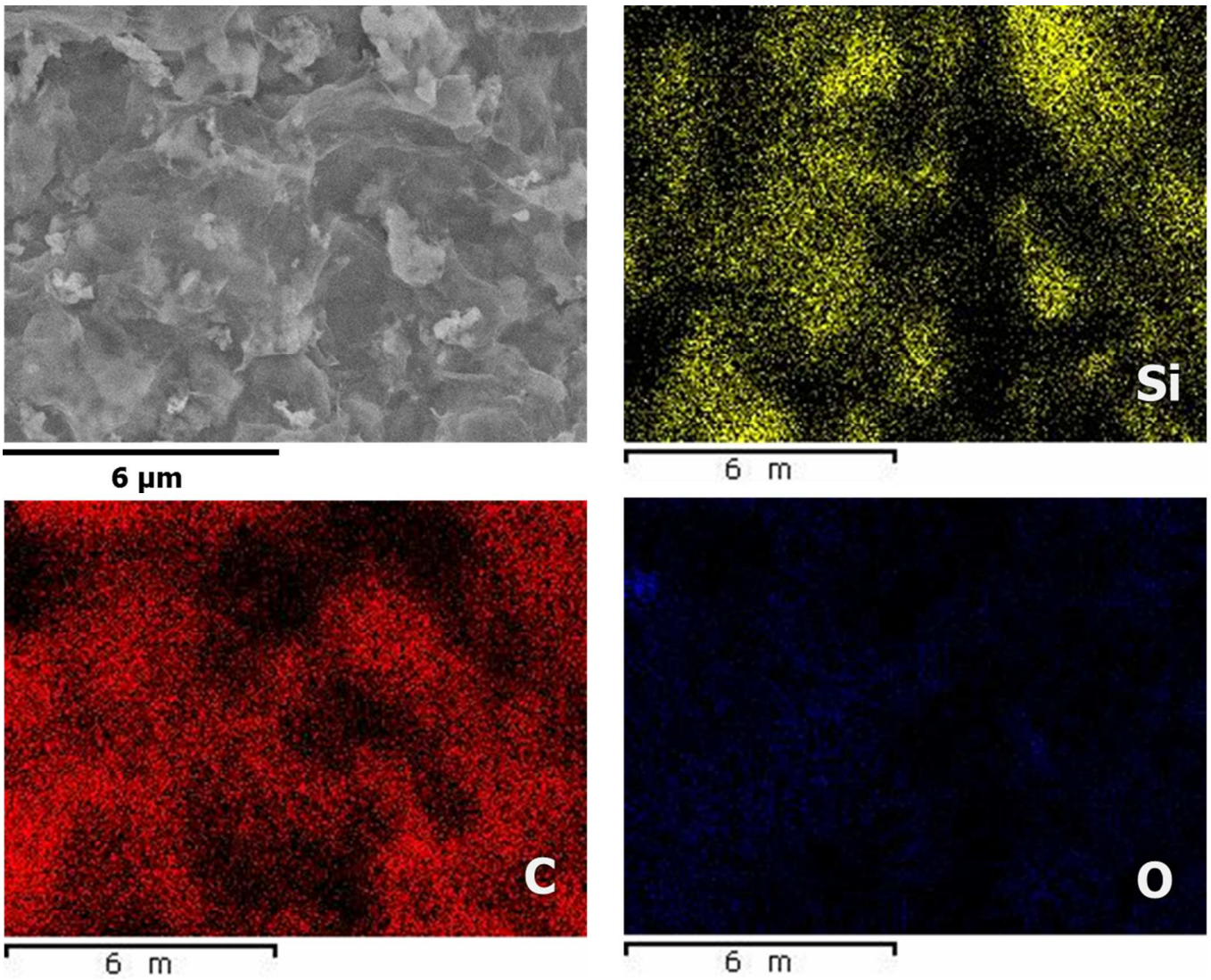

Fig. 5 A low magnification SEM image of RH-Si NPs -rGO composite with the corresponding EDS elemental maps

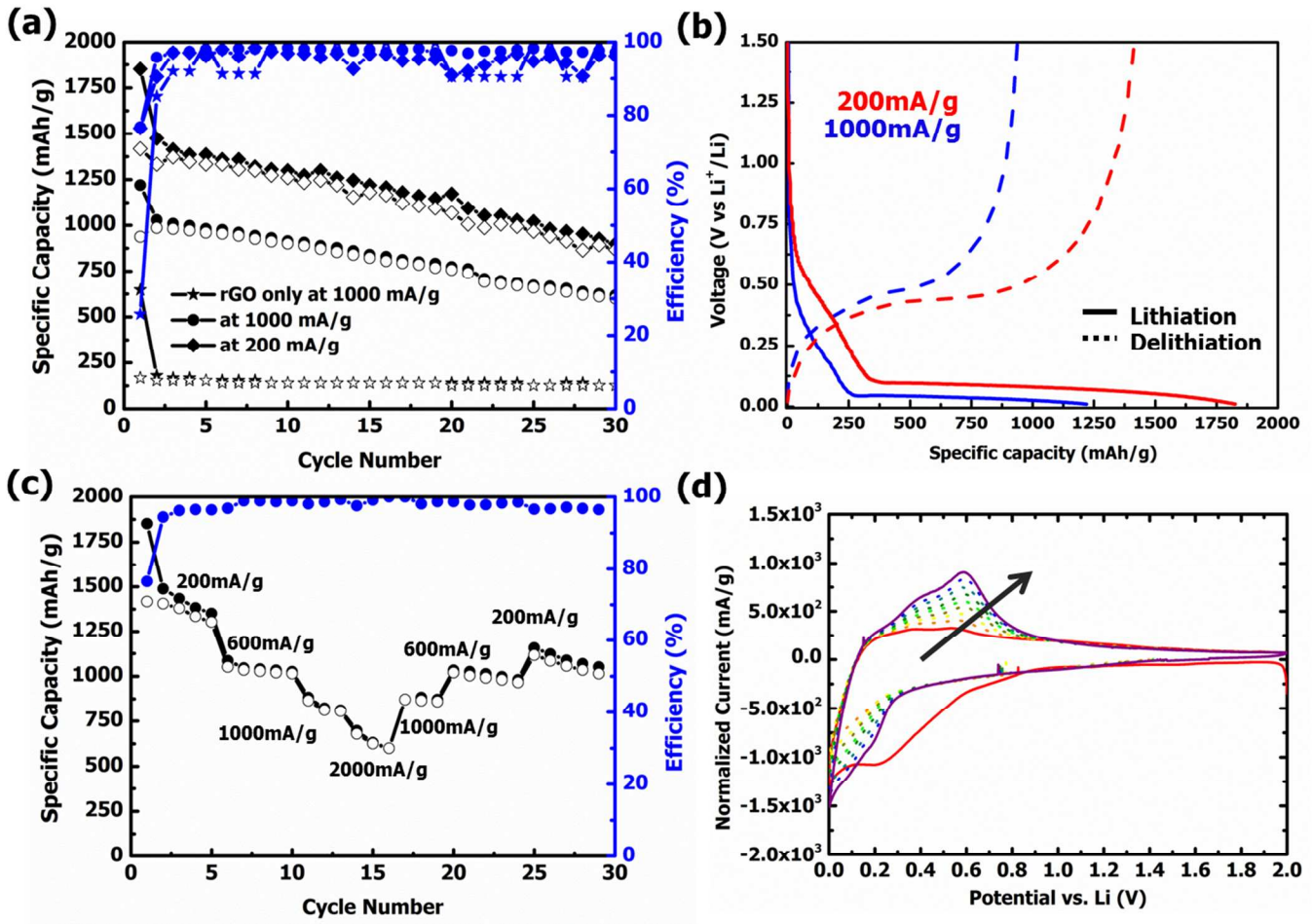

Fig. 6 (a) Cycling performance of the RH-Si NPs -rGO composite at indicated cycling rate with the corresponding performance of sample using rGO only for reference (close symbol – lithiation and open symbol – delithiation); (b) 1st charge and discharge cycle of the composite at various cycling rate (red for 200 mA/g and blue for 1000 mA/g); (c) Rate capability of the composite and (d) cyclic voltammogram of the composite at sweeping rate of 0.5mV/s and done at 10 cycles (arrow indicates direction from the 1st cycle to the 10th cycle).